Self-Consistent Density Functional Approach to a Metal/Electrolyte Solution Interface

A. A. Kornyshev*+, M. B. Partenskii**, and W. Schmickler+

Z. Naturforsch. **39a**, 1122–1133 (1984); received May 16, 1984

Two models for a plane interface between a free electron metal and a concentrated solution of a surface inactive electrolyte are treated fully self-consistently, taking into account both the polarizability of the metallic electron cloud and the reorientation of solvent molecules. The interfacial capacity is calculated as a function of the electrode charge, and its dependence on various system parameters is investigated. Some conclusions on the structure of the interface are drawn from a comparison between our results and experimentally observed trends.

§1. Introduction

The differential capacity of the metal/electrolyte interface is very sensitive to the structure of the contact region. It is analogous to the capacity of metal-insulator-metal systems, which contain both an interfacial and a 'geometric' contribution:

$$\frac{1}{C}=\frac{1}{C_{\text{int}}}+\frac{4\pi L}{\varepsilon}, \tag{1.1}$$

where L is the distance between the metal plates. Since, normally, $L > 10^4$ Å, the second term dominates, and the interfacial contribution is hardly seen. In the metal/electrolyte system, the ionic diffuse layer plays the role of the second metal plate, so that, at the point of zero charge (p.z.c.), the Debye length $\varkappa^{-1}$ takes the place of L in (1.1). Since $\varkappa^{-1}$ can be of the order of 10 Å or so, both terms are of the same order of magnitude, and the interfacial contribution to the capacity can be extracted from the experimental results.

For systems with no specific adsorption of ions, Grahame [1] proposed the general ansatz

$$\frac{1}{C}=\frac{1}{C_{\text{H}}}+\frac{1}{C_{\text{diff}}}, \tag{1.2}$$

where C_{H} is the interfacial (Helmholtz or inner layer) capacitance, which does not depend upon the electrolyte concentration but possibly depends on the electrode charge. C_{diff} is the ionic space charge capacitance in a dielectric continuum of dielectric constant ε, which is given in the Gouy-Chapman theory. Close to the p.z.c., $C_{\text{diff}}=\varepsilon\varkappa^{-1}/4\pi$; for large surface charge densities σ on the electrode, and, for example, for a binary 1-1 electrolyte of concentration c, this theory gives $C_{\text{diff}}=e/kT\theta c^{1/2}\ (1+\sigma^2/4\theta^2 c)$, where θ is a constant depending on solvent properties and temperature (for water at 25 °C, $\theta=0.0586$ C m^{-2} l$^{1/2}$ mol$^{-1/2}$).

Grahame's ansatz was used for 30 years for the parametrization of capacitance data. It worked successfully for so many systems that frequently the capacitance data were presented directly in the form of $C_{\text{H}}(\sigma)$ dependence. Reviews of such $C_{\text{H}}(\sigma)$ characteristics for various metal/solvent systems can be found, e.g. in Fawcett [2], Payne [3] and Frumkin [4].

Special attention to the verification of Grahame's hypothesis is paid in the recent review by Vorotyntsev [5].

Recently, Kornyshev, Schmickler and Vorotyntsev [6], and Kornyshev and Vorotyntsev [7] (for the region near the p.z.c., and for moderate charges, resp.), have given a theoretical foundation for Grahame's parametrization. They obtained rigorous criteria which limit the validity of the ansatz to low electrolyte concentrations ($c < 0.1$ M) and moderate charges ($\sigma < 10\ \mu$C cm^{-2}). An expression was found that relates C_{H} to the unified dielectric function $\varepsilon(z, z'; \sigma)$ (of an arbitrary form) of the metal/solvent system. Approximations for $\varepsilon(z, z'; \sigma)$ give corresponding expressions for C_{H}.

In the limit of high electrolyte concentrations ($c \gtrsim 1$ M), the contribution of the diffuse layer is so small that $1/C \approx 1/C_{\text{H}}$. Although the data for C_{H}

* Institute of Electrochemistry, Academy of Sciences of the USSR, Moscow, USSR, permanent address.
+ Reprint requests to Prof. W. Schmickler, Institut für Physikalische Chemie II, Universität Düsseldorf, D-4000 Düsseldorf, FRG.
** Physics Department, Ural High-School of Forest Technology, Sverdlovsk, USSR.

0340-4811 / 84 / 1100-1122 $ 01.30/0. – Please order a reprint rather than making your own copy.

obtained from concentrated solutions and those extrapolated from dilute solutions need not necessarily coincide, they normally agree well. The form of the $C_H(\sigma)$ characteristics is a mystery that still challenges the theoreticians. The pioneering work of Watts-Tobin [8] and the programme paper of Mott and Watts-Tobin [9] opened a 20 year history of 'molecular modelling' of the inner layer (for latest reviews see, e.g., Fawcett [2] and Rangarajan [10]).

However, in these molecular models, the metal was regarded as a region of constant potential. Thus, this approach appear to be incompatible with the modern electronic theory of metal surfaces (see, e.g., Lang [11] and Partenskii [12, 13]). In particular, studies of a metal surface in an external field (Teophilou and Modinos [14], Partenskii and Smorodinskii [15], Partenskii et al. [16]) revealed a considerable polarizability of the electron cloud near the interface when fields of the order of 1 V $Å^{-1}$, which is the typical order of magnitude for the metal/electrolyte interface, are applied. So the early arguments of Mott and Watts-Tobin [9], that the strong dependence of C_H on the electrode charge demonstrates that the capacity cannot be associated with the "metal electronic double layer", are no longer convincing. It is evident now that the complicated capacity-charge characteristics are the result of all the factors involved in the dielectric response of the interface: the polarizability of the solvent molecules, the response of the electronic cloud, and the strong interaction of these two subsystems.

Parsons [17] proposed a useful classification of $C_H(\sigma)$ curves (see the schematic plots in Fig. 1); many examples fitting into this scheme were discussed by Fawcett [2]. Type I is characterized by a central maximum and two minima. It is observed for the Hg/H_2O interface, and similarly for Cd and Pb. Type II displays a single maximum with no other extrema in the observable polarizable range of the electrode (the interfaces of Hg with cyclic carbonates, nitromethane, and DMSO). Type III has only a shallow minimum (Hg/MeOH, Hg/ethylenglycol, Hg/some aprotic solvents). Type IV refers to monotonic curves (e.g. Hg/acetonitrile).

Looking at these curves, one comes to the following conclusion:

1) the shape of the curve, and sometimes its type, depends strongly on both the metal and the contacting solvent (see Figure 1).

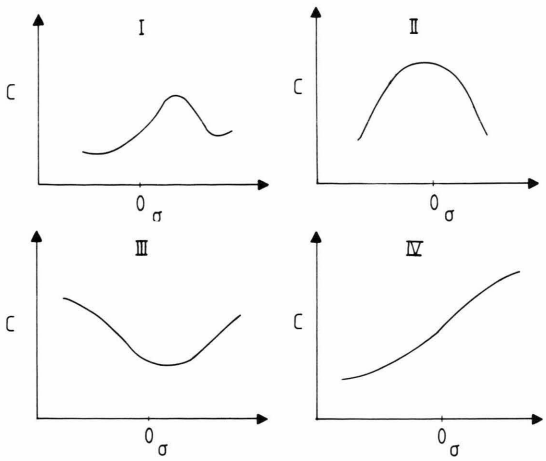

Fig. 1. Four different types of capacity-charge characteristics.

2) All four types have two features in common:
   a) C_H rises monotonically with σ near the p.z.c. (except for Hg/formamide).
   b) The curves obtained for a given solvent but for different metals converge at high negative potentials, so that the limiting branch $C(\sigma \to -\infty)$ depends solely on the solvent.

While these different types could be described by molecular models of the solvent, the problem of the influence of the metal was not solved. So, at present, it is natural to try to build an electronic theory of the metal/polar solvent interface, treating self-consistently both the metallic and the solvent components of the polarization.

A first attempt of this kind was made by Badiali, Rosinberg and Goodisman [18] (BRG), who treated the solvent as a dielectric continuum. The BRG model is an extension of the earlier works of Hirabayashi [19a] and Partenskii and Kuzema [19b] on the metal/insulator interface. In addition to the interaction of the electron with the polarizability of the solvent they also accounted for the repulsion of the metal electrons from the occupied orbitals of the solvent by introducing corresponding pseudopotentials. Also, they introduced a vacuum gap between the surface of the positive background, whose thickness they identified with the radius of the metal ions. This construction is in contradiction to the usual interpretation of the jellium model, where the surface of the positive background is identified with the surface plane touching the ionic spheres of the

first layer of metal ions. BRG applied their theory to the Hg/water and Ga/water interfaces, which experimentally exhibit type I capacity curves. However, their model gives type IV curves, and it also fails to reproduce the general features 2a and 2b noted above.

The next work was due to Schmickler [20], who combined his own two-dimensional molecular model for the solvent in the Helmholtz layer (Schmickler [21, 22]) with the Partenskii and Smorodinskii [15] modification of the Smith [23] jellium model. Schmickler's work helps to understand the following features of the system:

(1) It demonstrates that the interfacial capacity depends both on the nature of the solvent and of the metal.
(2) It correctly predicts capacity maxima (humps) for watertype solvents; the magnitude of the hump depends on the properties of the metal.
(3) The magnitude of the hump in his model decreases with temperature in agreement with Grahame's results for the Hg/water system [1 b].

His work, however, does not predict exactly the proper position of the hump. It is also limited to the purely electrostatic interaction of the point dipoles and the metal jellium; the treatment is dominantly numerical.

In this paper, we treat two one-dimensional models of the interface, involving both the polarizability of the electronic cloud and the reorientation of solvent molecules. The simplicity of the models will allow us to develop an analytical version of the theory helping to understand some basic effects prior to a variational calculation. Starting from these simplified models, we consider the interaction of the electronic polarizability and the orientational dipole polarizability, and their effect on the $C_H(\sigma)$ curves. The comparison of our calculated curves with experiment will help us to outline the shortcomings of present models, and indicate the direction of future research.

§2. Two Models for the Surface Layer of Molecules Bounding the Metal

Figure 2 gives a simplified picture of a water molecule, appropriate for our modelling of the interface. The picture was suggested by Schuster

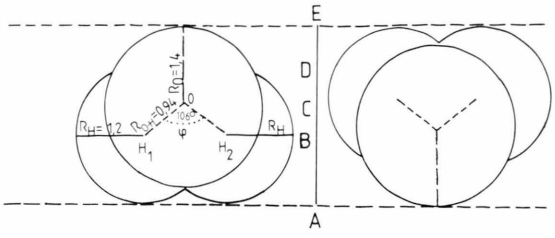

Fig. 2. Model of a water molecule after Schuster (1974) in the H, OH_2-plane. Distances: AB = 1.2 Å, CB = 0.56 Å, AD = 1.84 Å, CE = 1.4 Å, AE = 3.3 Å.

[24] on the basis of quantum-chemical calculations. We consider two models of the boundary layer, reflecting the given model of a water molecule. They have a common feature: The charge distribution in the plane parallel to the interface is assumed to be continuous and uniform. However, they are complementary, since one overemphasizes the discrete character of the distribution of the charge in the direction normal to the interface, while the other is based on the assumption of a smooth Lang [25] -layer like distribution. The first model reflects the shift in the position of the oxygen atoms with the inversion of the molecule, while the second model neglects completely any changes in the charge distribution in the course of molecular reorientation. In so far, we label these models as "discrete" (d-)model and "continuous" (c-)model, respectively.

2.1. *d-model* (Fig. 3)

The plane $z = a$ indicates the location of the negative charges due to the oxygen atoms of the molecules oriented to the surface with the oxygen

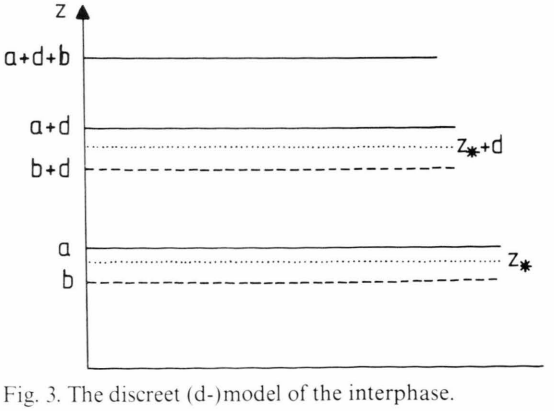

Fig. 3. The discreet (d-)model of the interphase.

end. Plane $z = a + d$: Positive charges due to hydrogen atoms of the molecules oriented with the oxygen end towards the surface.

Plane $z = b$: Positive charges due to the molecules oriented with the protons towards the surface.

Plane $z = b + d$: Negative charges due to molecules oriented with the protons towards the surface.

To reflect Schuster's picture of a water molecule, one should attribute the following values to these parameters:

$$a = R_0 = 2.64 \text{ a.u.}, \tag{2.1}$$

$$b = R_H = 2.26 \text{ a.u.}, \tag{2.2}$$

$$d = R_{0H} \cos(\varphi/2) = 1.07 \text{ a.u.} \tag{2.3}$$

We denote by N the total number of water molecules per surface area. γ is the fraction of molecules oriented with the oxygen end towards the surface, so that $(1-\gamma)$ is the fraction oriented with the protons towards the metal. $\gamma = 1/2$ corresponds to the case of no preferential orientation.

In the subsequent electrostatic calculations, it will be difficult to deal with four charged planes. To reduce the number of planes, we introduce two effective planes $z = z_*$ and $z = z_* + d$, where

$$z_* = \gamma a + (1-\gamma) b, \tag{2.4}$$

simulating Schuster's picture, i.e. for the above given values of the parameters, $a - b \approx 0.2$ Å, which is about 15% of a. With this choice, the effect of the variation of z_* with γ is not important.

Thus a charge, giving rise to a surface charge density

$$\Sigma = (1-2\gamma)\, qN \tag{2.5}$$

is smeared out in the plane z_*, with the charge $-\Sigma$ in the plane $z_* + d$. The coefficient q characterizes the separation of the charge in a water dipole: $0 < q < 1$.

The interaction of the molecular layer with the metal will not only be due to the charges on these planes, but also due to the Harrison-pseudopotential repulsion. The Harrison pseudopotential planes will be attributed directly to $z = a$, $z = b + d$ (repulsion from the oxygen cores) and $z = b$, $z = a + d$ (exchange repulsion from the electrons around the protons).

The region outside the full Van der Waal's distance AE (Fig. 2),

$$L = a + d + b, \tag{2.6}$$

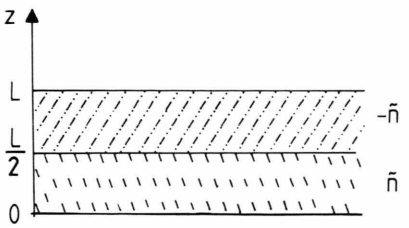

Fig. 4. The continuous (c-)model of the interphase.

is assumed to be filled with the concentrated electrolyte. The ionic diffuse layer effects will be neglected, and the region $z > L$ will be regarded as a region of constant potential ($\Phi = 0$).

2.2 c-model (Fig. 4)

The model is pictured in Figure 4. The ionic skeleton of the metal ($z < 0$) is separated from the concentrated electrolyte region ($z > L$) by two slaps of uniform charge density $\tilde{n}$ $(0 < z < L/2)$ and $-\tilde{n}$ $(L/2 < z < L)$:

$$\tilde{n} = qN(1-\gamma)\, 2/L - qN/L = \frac{qN}{L}(1-2\gamma) = \frac{\Sigma}{L}. \tag{2.7}$$

The meaning of q, N, and γ is the same as in the d-model. According to (2.7) the two slaps represent oxygen and hydrogen "subliquids". Each of these subliquids is characterized by different Harrison pseudopotentials, simulating the exchange repulsion of the metallic electron from the cloud of electrons surrounding the proton and the oxygen core electrons. This will be taken into account explicitely in the corresponding energy terms.

2.3 Discussion

The d-model overemphasizes the discreteness, the c-model stresses the smoothness of the charge distribution in the interfacial solvent layer. Our aim is to perform calculations for both models and to compare the results. If they occur to be qualitatively similar, this would mean that their common features ("two level behaviour") forms the essence of the dielectric response of the system.

We ascribe to the region $0 < z < L$ some dielectric screening due to the higher frequency degrees of freedom other than the orientational motions of the molecules. This will be represented by an effective dielectric constant ε_*; the value of ε_* may be

even smaller than the bulk high frequency dielectric constant (~ 6) due to effects of spatial dispersion (Vorotyntsev and Kornyshev [26]).

We finally note that the d- and c-models (especially the d-model), though elaborated for the case of water, may be more appropriate for some other solvents with reorientation of dipoles. Then γ will be an occupation parameter for this "two-level" system, and the "oxygen" and "hydrogen" terminology must be replaced by other appropriate terms.

§3. Adiabatic Energy Functional

In our one-dimensional picture the only "coordinate" characterizing the dipole motion is the occupation parameter γ. Since the movements of this orientational subsystem are much slower than the movements of the electrons of the metal, we may first solve the electronic problem for a fixed value of γ. In particular, we thereby obtain the surface energy as a function of γ (adiabatic surface energy term). In doing so, the electronic problem may be solved within the ground state formalism, since the low-energy fluctuations of γ cannot induce electronic transitions to excited states.

Thus, we shall use a modification of the density-functional formalism (Lang [11]), where the equilibrium values of the parameters are found by the minimization of the surface energy with respect both to the electronic density distribution $n(z)$ and the orientational subsystem parameter γ. We thus find *self-consistent* values of $n(z)$ and γ^*.

The energy functional of the electronic density which we use is

$$E = E_\gamma^{\mathrm{es}}[n] + E_\gamma^{\mathrm{H}}[n] + E_{\mathrm{m}}^{\mathrm{ps}}[n] + G[n] + E_\gamma^{\mathrm{ch}}, \qquad (3.1)$$

where the terms are specified below. (Throughout the paper, we use atomic units $e = \hbar = m_e = 1$, unless stated otherwise.)

3.1. *Electrostatic energy, $E_\gamma^{es}[n]$*

This is the only term depending on the solvent model used (*d* or *c*).

* The philosophy of this approach is similar to the adiabatic treatment of Hietschold et al. [27] of the lattice relaxation at metal surfaces where the variational parameter additional to those involved in $n(z)$ was the interlayer spacing between the last two planes of the ionic skeleton.

d-model

$$E_\gamma^{\mathrm{es}}[n] = -\tfrac{1}{2}\int_{-\infty}^{0} \mathrm{d}z\, \Phi(z)\,[n(z) - n_+] - \tfrac{1}{2}\int_{0}^{L} \mathrm{d}z\, \Phi(z)\, n(z) + \tfrac{1}{2}[\Phi(z_*) - \Phi(z_* + d)]\,\Sigma, \qquad (3.2)$$

where n_+ is the uniform positive background charge density of the metal (the ionic skeleton in the *jellium* model); and $\Phi(z)$ is the electric potential produced by all the charges in the system, obeying the following set of equations:

$$\Phi(z) = \begin{cases} \Phi_0(z) & z < 0, \\ \Phi_1(z) & 0 < z < z_*, \\ \Phi_2(z) & z_* < z < z_* + d, \\ \Phi_3(z) & z_* + d < z < L; \end{cases} \qquad (3.3)$$

$$\Phi_0'' = \frac{4\pi}{\varepsilon_{\mathrm{M}}}(n - n_+), \quad z < 0;$$

$$\Phi_1'' = \frac{4\pi}{\varepsilon_*} n, \qquad 0 < z < z_*;$$

$$\Phi_2'' = \frac{4\pi}{\varepsilon_*} n, \qquad z_* < z < z_* + d;$$

$$\Phi_3'' = \frac{4\pi}{\varepsilon_*} n, \qquad z_* + d < z < L; \qquad (3.4)$$

$$\Phi_0(0) = \Phi_1(0), \quad \varepsilon_{\mathrm{M}}\Phi_0'(0) = \varepsilon_*\Phi_1'(0),$$

$$\Phi_1(z_*) = \Phi_2(z_*), \quad \Phi_1'(z_*) = \Phi_2'(z_*) + \frac{4\pi}{\varepsilon_*}\Sigma,$$

$$\Phi_2(z_* + d) = \Phi_3(z_* + d), \quad \Phi_2'(z_* + d) = \Phi_3'(z_* + d) - \frac{4\pi}{\varepsilon_*}\Sigma,$$

$$\Phi_3(L) = 0, \quad \Phi_0(-\infty) = \mathrm{const}, \qquad (3.5)$$

where ε_{M} is the high-frequency ionic skeleton dielectric constant, – its value is normally close to unity – (for the discussion of this quantity see the review articles by Hodgson [2] and Vorotyntsev and Kornyshev [28]).

c-model

$$E_\gamma^{\mathrm{es}}[n] = -\tfrac{1}{2}\int_{-\infty}^{0} \mathrm{d}z\, \Phi(z)\,[n(z) - n_+] - \tfrac{1}{2}\int_{0}^{L/2} \mathrm{d}z\, \Phi(z)\,[n(z) - \hat{n}] - \tfrac{1}{2}\int_{L/2}^{L} \mathrm{d}z\, \Phi(z)\,[n(z) + \hat{n}], \qquad (3.6)$$

where Φ obeys the equations:

$$\Phi = \begin{cases} \Phi_0(z), & z < 0, \\ \Phi_1(z), & 0 < z < L/2, \\ \Phi_2(z), & L/2 < z < L, \end{cases} \tag{3.7}$$

$$\Phi_0'' = \frac{4\pi}{\varepsilon_M}(n - n_+), \quad z < 0,$$

$$\Phi_1'' = \frac{4\pi}{\varepsilon_*}(n - \tilde{n}), \quad 0 < z < L/2,$$

$$\Phi_2'' = \frac{4\pi}{\varepsilon_*}(n + \tilde{n}), \quad L/2 < z < L, \tag{3.8}$$

$$\Phi_0(0) = \Phi_1(0), \quad \varepsilon_M \Phi_0'(0) = \varepsilon_* \Phi_1'(0), \tag{3.9}$$
$$\Phi_1(L/2) = \Phi_2(L/2), \quad \Phi_1'(L/2) = \Phi_2'(L/2).$$

3.2. *Harrison pseudopotential energy*

d-model

$$E_\gamma^H = N\{\Lambda\gamma n(a) - \lambda\gamma n(a+d) + \lambda(1-\gamma) n(b) + \Lambda(1-\gamma) n(l+d)\}, \tag{3.10}$$

where λ and Λ are the characteristic intensities of the Harrison pseudo-potential for positive and negative ends of the molecules of the dipole layer.

c-model

$$E_\gamma^H = \frac{N}{L}\left\{B\int_0^L dz\, n(z) + 2D(1-\gamma)\int_0^{L/2} dz\, n(z) + 2D\gamma\int_{L/2}^L dz\, n(z)\right\}, \tag{3.11}$$

where B is the intensity of the Harrison pseudo-potential of the negative "subliquid", and D of the positive one.

It is possible to add to (3.10) or (3.11) the terms responsible for the repulsion from the closed shell electrons of the medium at $z > L$ (ions and dipoles of the concentrated electrolyte). However $n(z)$ is normally negligible at $z > L$, and these terms may be ignored.

3.3. *Pseudo-potential correction inside the metal*

$$E_m^{ps}[n] = C\int_{-\infty}^0 dz\,[n(z) - n_*]. \tag{3.12}$$

This is a semi-empirical term, responsible for the deviation from the jellium model. C is a constant, different for each metal and crystal orientation, fitted by the comparison of the calculated vacuum work function with the corresponding experimental values. With the help of this term, one may formally come to the limit of an infinite potential barrier for electrons at the metal surface ($C \to -\infty$).

3.4. *Kinetic-exchange-correlation energy*

For this quantity we use the standard local density approximation with the gradient correction to the kinetic energy term only (Smith [23]):

$$G[n] = G_{kin} + G_x + G_c + G_{inh}, \tag{3.13}$$

$$G_{kin} = 0.3(3\pi^2)^{2/3}\int_{-\infty}^{\infty} dz\,[n^{5/3}(z) - n_+^{5/3}\theta(-z)], \tag{3.14}$$

$$G_x = -0.75\left(\frac{3}{\pi}\right)^{4/3}\int_{-\infty}^{\infty} dz\,[n^{4/3}(z) - n_+^{4/3}\theta(-z)], \tag{3.15}$$

$$G_c = -0.056\int_{-\infty}^{\infty} dz\left[\frac{n^{4/3(z)}}{0.079 + n^{1/3}(z)} - \frac{n_+^{4/3}\theta(-z)}{0.079 + n_+^{1/3}}\right], \tag{3.16}$$

$$G_{inh} = \frac{1}{72}\int_{-\infty}^{\infty} dz\,\frac{1}{n(z)}\left(\frac{dn}{dz}\right)^2. \tag{3.17}$$

3.5. *Chemical energy*

E_γ^{ch} is responsible for the interactions of the molecules of the surface layer with the degrees of freedom of the substrate other than free electrons (e.g. chemical binding with d-orbitals) and the short range interactions between the molecules, which are not screened or perturbed by the electronic cloud spilling over the skeleton edge. Thus this term is independent of n. A simple approximation is

$$E_\gamma^{ch} = \gamma N \Delta, \tag{3.18}$$

where $\Delta < 0$ and $\Delta > 0$ correspond to the preferential orientation of molecules with their negative and positive ends, respectively, towards the surface.

§4. Electrode Charge Equation

The charge density σ on the electrode is related to the electronic density $n(z)$ through the relation

$$\int_{-\infty}^{+\infty} dz\,[n(z) - n_*\theta(-z)] = \sigma. \tag{4.1}$$

§5. Minimization Procedure

In order to find the equilibrium (in fact, the ground state) values of $n(z)$ and γ, we minimize the surface energy given by (3.1) with respect to these quantities. In doing so we use the trial function approach. A simple set of trial functions is

$$n(z) = n_+ \begin{cases} 1 - \dfrac{\beta}{\alpha+\beta} e^{\alpha z}, & z < 0, \\ \dfrac{\alpha}{\alpha+\beta} e^{-\beta z}, & z \geqq 0, \end{cases} \tag{5.1}$$

where, according to (4.1),

$$1/\alpha - 1/\beta = \sigma/n_+ . \tag{5.2}$$

Thus (5.1) and (5.2) provide a one-parameter set of trial functions. More complicated trial functions can also be used, but they lead to more cumbersome expressions. They will not be considered in this work, since we aim to obtain simple analytical results.

5.1. Electrostatic energy

The solution of the electrostatic Eqs. (3.3)–(3.5) for the d-model and (3.6)–(3.9) for the c-model, with $n(z)$ given by (5.1), is:

$$E_\gamma^{\mathrm{es}} = \frac{2\pi L}{\varepsilon_*}\sigma^2 + E_\gamma^{\mathrm{es}} + \frac{2\pi}{\varepsilon_*} \cdot \begin{cases} 2\sigma\Sigma d + \Sigma^2 d + \dfrac{2n_+\Sigma\alpha}{\beta^2(\alpha+\beta)} e^{-\beta z_*}(1 - e^{-\beta d}) & \text{d-model}, \\ \dfrac{1}{2}\sigma\Sigma L + \dfrac{1}{12}\Sigma^2 L + \dfrac{2n_+\Sigma\alpha}{\beta^3(\alpha+\beta)L}(1 - e^{-\beta L/2})^2 & \text{c-model}, \end{cases} \tag{5.3}$$

where the electrostatic energy of the charged jellium is

$$E_\gamma^{\mathrm{es}} = \frac{\pi n_+^2}{\beta(\alpha+\beta)^2}\left\{\frac{\beta^3}{\varepsilon_M \alpha^3} + \frac{1}{\varepsilon_*}\left(4 - 3\frac{\alpha^2}{\beta^2}\right) + \frac{1}{\varepsilon_*} e^{-\beta L}\frac{4(\alpha^2-\beta^2) - \alpha^2 e^{-\beta L}}{\beta^2}\right\}. \tag{5.4}$$

The first term in (5.3) is the energy of a plane capacitor with a capacitance $\varepsilon_*/4\pi L$. The difference between the two models is seen in the terms describing the interaction of the jellium with a surface solvent layer, the electrostatic self-energy of the bi-layer, and the interaction of the bi-layer with a net charge σ.

5.2. Harrison pseudo-potential energy

$$E_\gamma^{\mathrm{H}} = N n_+ \frac{\alpha}{\alpha+\beta} \begin{cases} 1\gamma e^{-\beta a} + \lambda\gamma e^{-\beta(a+d)} + \lambda(1-\gamma) e^{-\beta b} + \Lambda(1-\gamma) e^{-\beta(b+d)} & \text{d-model} \\ \dfrac{1}{\beta L}[B + 2D(1-\gamma) + 2D(2\gamma-1) e^{-\beta L/2} - (B + 2\gamma D) e^{-\beta L}] & \text{c-model}. \end{cases} \tag{5.5}$$

5.3. Metal pseudo-potential correction

$$E_{\mathrm{m}}^{\mathrm{ps}} = -C n_+ \frac{\beta}{\alpha(\alpha+\beta)}. \tag{5.6}$$

5.4. Kinetic-exchange-correlation jellium energy

$$G_{\mathrm{kin}} = 3P_1 \frac{n_+^{5/3}}{\alpha}\left[R_1(t_0) - R_1(1) + 0.2\frac{\alpha}{\beta} t_0^5\right], \tag{5.7}$$

$$G_{\mathrm{x}} = 3P_2 \frac{n_+^{4/3}}{\alpha}\left[R_2(t_0) - R_2(1) + 0.25\frac{\alpha}{\beta} t_0^4\right], \tag{5.8}$$

$$G_{\mathrm{c}} = 3P_3 \frac{n_+}{\alpha}\left\{R_3(t_0) - R_3(1) + \frac{\alpha}{\beta}[R_4(t_0) - R_4(0)]\right\}, \tag{5.9}$$

$$G_{\mathrm{inh}} = P_4 n_+ \ln\frac{\alpha+\beta}{\alpha}, \tag{5.10}$$

where

$$t_0 = \left(\frac{\alpha}{\alpha+\beta}\right)^{1/3}, \tag{5.11}$$

$$P_1 = 0.3(3\pi^2)^{2/3}, \quad P_2 = -0.75\left(\frac{3}{\pi}\right)^{1/3},$$

$$P_3 = -0.056, \qquad P_4 = \frac{1}{72}, \tag{5.12}$$

$$R_1(t) = t^5/5 + t^2/2 - 0.5\ln(1 + t + t^2) + \frac{1}{\sqrt{3}}\operatorname{arctg}\frac{2t+1}{\sqrt{3}}, \tag{5.13}$$

$$R_2(t) = t^4/4 + t - 0.5\ln(1 + t + t^2) - \frac{1}{\sqrt{3}}\operatorname{arctg}\frac{2t+1}{\sqrt{3}}, \tag{5.14}$$

$$R_3(t) = t^3/3 - st^2/2 + s^2 t - \frac{s^6}{s^3+1} \ln(t+s) - \frac{s(s-1)}{2(s^3+1)} \ln(1+t+t^2) - \frac{s}{\sqrt{3}(1-s+s^2)} \operatorname{arctg} \frac{2t+1}{\sqrt{3}}, \tag{5.15}$$

$$R_4(t) = t^3/3 - st^2/2 + s^2 t - s^3 \ln(t+s), \tag{5.16}$$

$$s = \frac{0.079}{n_+^{1/3}}. \tag{5.17}$$

Now $E = E\left(\beta, \gamma, \sigma, n_+, N, q, \underset{B,\ D}{L,\ z_*,\ d,\ \Lambda,\ \lambda}, C\right)$ is a function of the two variational parameters β and γ, with the other parameters being fixed. Observable quantities are calculated for the values $\beta = \beta_{\min}$ and $\gamma = \gamma_{\min}$, which provide the absolute minimum of E in the range of $0 < \gamma < 1$.

§6. Calculation of Observable Quantities

The equilibrium interfacial potential drop

$$V = \Phi(-\infty) - \Phi(L) = \Phi(-\infty) \tag{6.1}$$

is equal to

$$V = \frac{4\pi L}{\varepsilon_*}\sigma + \frac{4\pi n_+}{(\alpha+\beta)\beta} \cdot \left[\frac{1}{\varepsilon_M}\frac{\beta^2}{\alpha^2} + \frac{\alpha}{\beta}\frac{1}{\varepsilon_*}(1-e^{-\beta L})\right] + \frac{4\pi}{\varepsilon_*} qN(1-2\gamma) \begin{cases} d & \text{d-model} \\ L/4 & \text{c-model} \end{cases}\Bigg|_{\substack{\beta=\beta\min \\ \gamma=\gamma\min}}. \tag{6.2}$$

This is not a measurable quantity. However, one can measure the differential capacity

$$C_H = d\sigma/dV. \tag{6.3}$$

According to (6.2):

$$\frac{1}{4\pi C_H} = \frac{L}{\varepsilon_*} + n_+ \frac{\partial}{\partial\sigma}\left\{\frac{\frac{1}{\varepsilon_M}\frac{\beta^2}{\alpha^2} + \frac{1}{\varepsilon_*}(1-e^{-\beta L})}{\beta(\alpha+\beta)}\right\} - \frac{2qN}{\varepsilon_*}\frac{\partial\gamma}{\partial\sigma} \begin{cases} d & \text{d-model}, \\ L/4 & \text{c-model}. \end{cases} \tag{6.4}$$

Simpler equations are found for the p.z.c., where $\sigma = 0$. Here, neglecting terms of the order $O(\exp(-\beta L))$, we have

$$V_{\sigma=0} = \frac{2\pi n_+}{\beta^2}\left(\frac{1}{\varepsilon_M} + \frac{1}{\varepsilon_*}\right) + \frac{4\pi qN}{\varepsilon_*}(1-2\gamma_{\sigma=0}) \begin{cases} d \\ L/4, \end{cases} \tag{6.5}$$

$$\frac{1}{4\pi C_H} = \frac{L-\beta^{-1}}{\varepsilon_*} + \left(\frac{5}{4\varepsilon_M} + \frac{3}{4\varepsilon_*}\right)\frac{1}{\beta} - \frac{\beta^1}{\beta^3} n_+ \left(\frac{1}{\varepsilon_M} + \frac{1}{\varepsilon_*}\right) - \frac{2qN}{\varepsilon_*}\gamma^1 \begin{cases} d \\ L/4. \end{cases} \tag{6.6}$$

§7. A Mechanism for the Resolution of the Rice Paradox

The Rice Paradox is discussed in detail in [6, 7, 26]: Any non-selfconsistent theory, with an infinite energy barrier at the interface, gives too large values for the inverse interfacial capacity; in other words: any model which does not allow for electron spill-over at the metal surface, is incompatible with experimental results. It was also demonstrated in these works (see also Vorotyntsev et al. [29]) that the penetration of the electrons into a solvent with a higher background dielectric constant ε_* reduces the calculated inverse capacity to the same order of magnitude as the experimental values.

From (6.6) we see that in our present model two terms exist which tend to make the inverse capacity smaller: the first term, which is proportional to β'/β^3, reflects the response of the jellium tail to the application of an external field. The electrons follow the field, thus reducing the potential drop across the interface (see also Schmickler [20]); in classical terms, this corresponds to a polarizability of the electronic system at the surface. This is a quantum-mechanical effect, which does not arise in theories with an infinite barrier at the surface; we shall see below that it reduces the inverse capacity to a reasonable magnitude, and thus resolves the Rice paradox. The other term is proportional to γ' and reflects the orientational polarization of the water on which the classical double layer theories had focused their attention.

§8. Results of Variational Calculations

The interfacial capacity is a complicated function of the various parameters of our model. Below, we

shall present results of model calculation for illustration. These plots can be understood by the following considerations:

The capacity-charge characteristics reflect the influence of the solvent, the metal, and their interaction; we shall discuss these three contributions:

a) *the solvent:* To understand the effect of the solvent, we discuss the capacity C_s of the solvent layer in the absence of the metal. For the c-model, we have

$$\frac{1}{4\pi C_s} = \begin{cases} L/4\varepsilon_* & \text{for } |\sigma| \leqq qN/3\,, \\ L/\varepsilon_* & \text{for } |\sigma| > qN/3\,. \end{cases} \tag{8.1}$$

For the d-model:

$$\frac{1}{4\pi C_s} = \begin{cases} (L-d)/\varepsilon_* & \text{for } |\sigma| \leqq qN\,, \\ L/\varepsilon_* & \text{for } |\sigma| > qN\,. \end{cases} \tag{8.2}$$

Thus, in both models C_s has a rectangular 'hump' centred at $\sigma = 0$. In the c-model, the width of the hump is smaller and, with $L \approx 4$ Å for water, its height is greater.

b) *the jellium:* The jellium capacity is determined by the variation of the inverse penetration lengths α and β with the charge density σ. This is a smoothly varying function, which decreases monotonically as one goes from negative charge densities to positive ones. The polarizability of the jellium (i.e. the variation of the surface dipole potential) increases with the electronic density n_+.

c) *The interaction terms:* At the p.z.c., the extension of the electron tail into the solvent produces a net orientation of the solvent layer with the negative oxygen-end towards the metal (i.e. $\gamma > 1/2$). This results in a shift of the capacity hump produced by the solvent towards negative charges.

The pseudopotential terms in (3.10) and (3.11) also reflect the strength of the interaction. Only positive values of B and D are physically meaningful, since they represent a repulsion of the electrons from the solvent. They tend to increase the inverse electron penetration lengths α and β, and decrease the polarizability of the jellium tail, leading to a smaller contribution of the jellium to the inverse capacity.

Finally, we note that for rough considerations the capacity can be split into a metal and a solvent term; however, it is the inverse capacity of the subsystems which are roughly additive.

In the numerical calculation we have generally taken: $L = 4$ Å for the thickness of the inner layer of the solvent, and $N = 10^{19}\,\mathrm{m}^{-2}$, in accord with the commonly accepted values for water, $\varepsilon_* = 6$, and $\varepsilon_M = 1$, unless otherwise stated. The choice of trial functions limits our calculations to fairly low charge densities, $|\sigma| \leqq 10\ \mu\mathrm{C/cm}^2$.

Since our results for the c-model are more interesting than for the d-model, we shall present the results for the former model first.

c-model

Dependence on q: The natural choice for q is gouverned by the consideration that qL should be equal to the dipole moment of the water molecule. This gives $q \approx 0.1$ a.u., and we shall use this value in the subsequent calculations. Still, it is of interest to see what effect q has on the capacity characteristics. This is shown in Fig. 5; here, we have set $B = C = D = \Delta = 0$, and chosen $n_+ = 0.0128$ a.u., which corresponds to mercury. For each value of q, we get a capacity curve with a roughly rectangular hump, centred at negative charges. The width of the hump is approximately $2qN/3$, and they are roughly centred at $\sigma = -0.2\ \mu\mathrm{C/cm}^2$. Due to the jellium, there is an underlying trend for the capacity to decrease with increasing σ.

Dependence on the metal: With increasing electronic density n_+, the dipole potential at the interphase, and also the variation of this dipole potential with the charge density, become greater. Hence the total interfacial capacity becomes larger with increasing n_+. This can be compared with the experimental observation that the capacity of second and third row sp-metals increases with the electronic density (Schmickler and Henderson [22a]). In addition, the interaction of the jellium tail with the

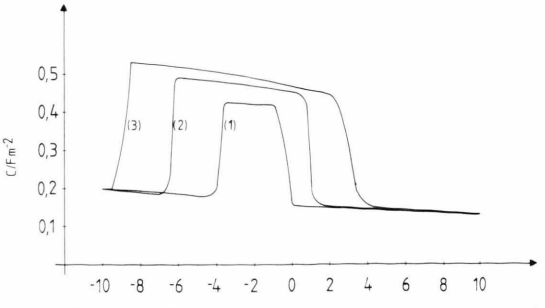

Fig. 5. Capacity-charge curves in the c-model; (1) $q = 0.02$ a.u., (2) $q = 0.06$ a.u., (3) $q = 0.1$ a.u.

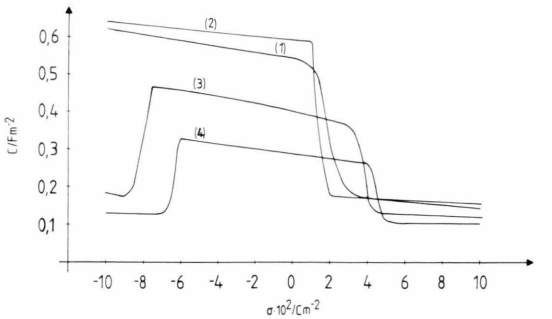

Fig. 6. Capacity-charge curves in the c-model; (1) $\varepsilon_M = 2$, $n_+ = 0.01$, $C = 0$; (2) $\varepsilon_M = 1$, $n_+ = 0.02$, $c = 0$; (3) $\varepsilon_M = 1$, $n_+ = 0.01$, $C = 0$; (4) $\varepsilon_M = 1$, $n_+ = 0.0128$, $C = -1.5$ eV; $B = D = \Delta = 0$ in all curves.

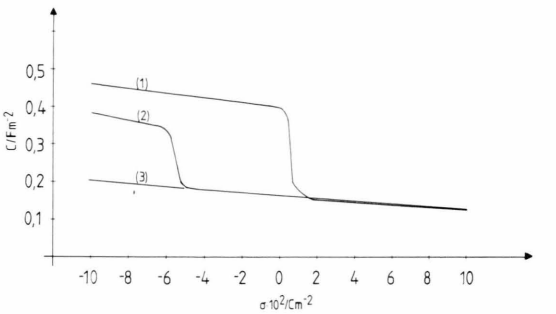

Fig. 7. Capacity-charge curves in the c-model; $n_+ = 0.0128$, $C = 0$; (1) $B = D = 0.2$ a.u.; (2) $B = D = 0.6$ a.u.; (3) $B = D = 2$ a.u.

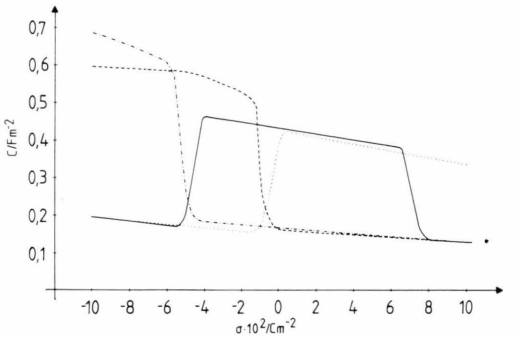

Fig. 8. Capacity-charge curves in the c-model; $n_+ = 0.0128$, $B = C = D = 0$. Full-line: $\Delta = 10^{-3}$ cm; (−−): $\Delta = -5 \cdot 10^{-4}$ a.u.; (−·): $\Delta = -10^{-3}$ a.u.

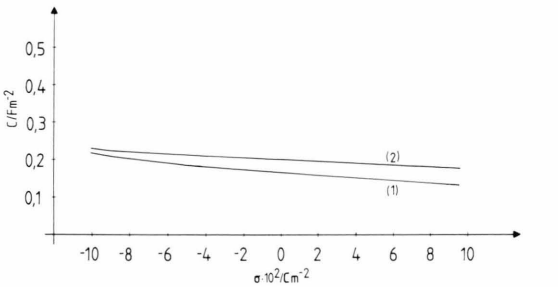

Fig. 9. Capacity-charge curves in the d-model; (1) $n_+ = 0.01$; (2) $n_+ = 0.02$.

solvent becomes stronger, and the capacity hump is shifted towards negative charge densities (see Figure 6).

Increasing the background dielectric constant ε_M of the metal has a similar effect: the extension of the jellium tail increases, and so does the capacity and the interaction with the solvent.

Similarly, the metal pseudopotential C will decrease the extension of the jellium tail, when it is negative, while a positive value of C will increase the penetration depth. This is illustrated by curve (4) in Fig. 6 for the case of mercury. There, the recommended value for C is -1.55 eV [30]; consequently, the interfacial capacity is decreased and the hump is shifted towards the p.z.c.

Harrison pseudopotentials

Inspection of (5.5) shows that the pseudopotential parameters B and D tend to push the jellium tail back into the metal, and that D favours a value of $\gamma = 1$. For reasonable orders of magnitude of B and D in the region of up to 1 a.u., the former effect is very small while the latter is pronounced. Figure 7 shows that with increasing values of D the hump is shifted towards negative charges, since $\gamma = 1$ is favoured; for $B = D = 1$ a.u. the hump is not in the investigated region.

Chemical energy

The chemical energy parameter Δ has an effect on the solvent orientation γ only: positive Δ favoures small γ, and the hump is shifted towards positive charges, while negative Δ favoures $\gamma = 1$, and thus shifts the hump towards smaller σ. This is illustrated in Figure 8.

d-model

Inspection of (5.3) shows that, with α and β of the order of 1 a.u., the interaction between the solvent and the jellium is stronger in the d-model than in

the c-model. The overall effect is to push the jellium tail back into the metal and to decrease the contribution of the jellium to the capacity. For reasonable values of q ($q \approx 0.1$ a.u.), the width of the solvent contribution is greater than the range of σ which we have investigated (cf. (8.2)). Hence, the calculated capacity curves give almost constant capacity in this range (see Figure 9). Again, the capacity becomes greater with increasing electronic density. Since for reasonable parameters the capacity curves are rather featureless, we shall not present more calculations for this model.

§9. Discussion

Comparing our calculated capacity-charge characteristics with the experimental curves classified by Parsons, we note that in agreement with type I and II our curves exhibit a capacity hump with a width of a reasonable order of magnitude. However, both the shape and the position of the hump are wrong: The roughly trapezoidal shape is but an imperfect representation of the smooth humps observed experimentally, and, except when the chemical interaction Δ is greater than zero (i.e. when the hydrogen interacts stronger with the metal than the oxygen end, which is unlikely from a chemical point of view), the centre of the hump is on the wrong side of the p.z.c.

The first defect is obviously caused by the simple solvent model which we employed. We expect that thermal effects, which are not included in our model, would smooth the edges of the hump. Also, the representation of the first water layer by a system of charges is certainly an oversimplification. The structure of water is largely determined by hydrogen bonding, and this will also effect its dielectric properties. An attempt to include hydrogen bonds into double layer modelling has been made by Guidelli [31]. However, the success of electrostatic water models like ST2 [32] shows that the effect of hydrogen bonding may partially be simulated by a judicious choice of the charge distribution.

In our model, both the metal and the solvent give appreciable contributions to the interfacial capacity. Thus, in contrast to the older classical model, the interfacial capacity depends strongly on the metal characteristics (see Fig. 7); so we can at least qualitatively account for the dependence of the double layer capacity on the nature of the metal. Also, in agreement with experimental evidence, at the p.z.c. our model predicts a preferential orientation of the oxygen end towards the metal. This is caused by the electronic tail extending into the solution, which generates a positive field at the metal surface at the p.z.c.

Recently, Carnie and Chan [33], and Blum and Henderson [34] have solved a model in which the electrolyte is represented as an ensemble of hard sphere ions and dipoles. The calculated wall-dipole correlation functions show an oscillatory behaviour over a range of several solvent diameters. Thus it seems that the solvent contribution to the inner layer capacity is not solely determined by the first layer of solvent molecules, like was we have supposed in our present work, but by a somewhat larger boundary region. Unfortunately, the solution has been obtained for small electrode charges only, so that the calculation of the interfacial capacity is limited to the p.z.c. Recently, the interphase has been modelled as an ensemble of hard sphere ions and dipoles in contact with jellium [22a, 35]. Qualitatively, the result of these works are similar to ours at the p.z.c.; in particular, they also predict an increase of the capacity with the electronic density.

§10. Conclusion

In this paper we have presented a fully self-consistent model of the interface between a metal, modelled as jellium, and a solvent layer, simulated by a system of charges. While the model can explain some qualitative features of the experimental capacity curves – the metal dependence, and the occurrence of a 'hump', – it still has serious defects which we hope to remedy in a future work.

Acknowledgement

One of us (A. A. K.) wishes to thank Prof. J. W. Schultze for his hospitality at the Institute of Physical Chemistry of the University of Düsseldorf, where the major part of this work was realized. He is also indebted for valuable discussions to Dr. M. A. Vorotyntsev at the Institute of Electrochemistry of the Academy of Sciences of the USSR in Moscow. A. A. K. and M. B. P. are thankful to Dr. V. E. Kuzema (from the Ural Polytechnic Institute) for useful discussion of the computer simulations. W. S. appreciates the support of the Deutsche Forschungsgemeinschaft.

[1] a) D. C. Grahame, Chem. Rev. **41,** 441 (1947), b) D. C. Grahame, J. Amer. Chem. Soc. **79,** 2093 (1957).
[2] W. R. Fawcett, Israel J. Chem. **18,** 3 (1979).
[3] R. Pain, Adv. Electrochem. Electrochem. Ing. **7,** 1 (1970).
[4] A. N. Frumkin, Zero Charge Potentials, Nauka, Moscow 1979 (in Russian).
[5] M. A. Vorotyntsev, in: "Modern Aspects of Electrochemistry" (1985), to be published.
[6] A. A. Kornyshev, W. Schmickler, and M. A. Vorotyntsev, Phys. Rev. B **25,** 5244 (1982).
[7] A. A. Kornyshev and M. A. Vorotyntsev, Canadian J. Chem. **59,** 2031 (1981).
[8] R. J. Watts-Tobin, Phil. Mag. **6,** 133 (1961).
[9] N. F. Mott and R. J. Watts-Tobin, Electrochim. Acta **4,** 79 (1961).
[10] S. K. Rangarajan, Chem. Soc. Specialist Periodical Reports, Electrochemistry Ser. **7** (1982).
[11] N. D. Lang, Solid State Phys. **28,** 225 (1973).
[12] M. B. Partenskii, Usp. Fiz. Nauk **128,** 69 (1979); Engl. transl.: Soviet Physics: Uspekhi.
[13] M. B. Partenskii, Poverkhnost, Ne **10,** 15 (1982).
[14] A. K. Theophilou and A. Modinos, Phys. Rev. B**6,** 801 (1972).
[15] M. B. Partenskii and Y. Smorodinskii, Fiz. tverd. Tela **16,** 644, Leningrad 1974.
[16] M. B. Partenskii, V. E. Kuzema, and V. I. Feldman, Izv. Vuvov. ser. fiz No. **11,** 10 (1981).
[17] R. Parsons, Electrochim. Acta **21,** 681 (1976).
[18] J. P. Badiali, M. B. Rosinberg, and J. Goodisman, J. Electroanal. Chem. **143,** 73 (1983).
[19a] Hirabayashi, Phys. Rev. B**3,** 4023 (1971).
[19b] M. B. Partenskii and V. E. Kuzema, Fiz. tverd. Tela **21,** 2842 (1979).
[20] W. Schmickler, J. Electroanal. Chem. **150,** 19 (1983).
[21] W. Schmickler, J. Electroanal. Chem. **149,** 15 (1983).
[22] W. Schmickler, J. Electroanal. Chem. **157,** 1 (1983).
[22a] W. Schmickler and D. Henderson, J. Chem. Phys. **80** (1984) in press.
[23] J. W. Smith, Phys. Rev. **181,** 522 (1969).
[24] P. Schuster, in: Structure of Water and Aqueous Solutions, ed.: W. Luck, Verlag Chemie, Weinheim 1974.
[25] N. D. Lang, Phys. Rev. V**4,** 4234 (1971).
[26] M. A. Vorotyntsev and A. A. Kornyshev, Elektrokhimiya **15,** 660 (1979).
[27] M. Hietschold, G. Paasch, and I. Bartos, Phys. Stat. Sol. (b) **101,** 239 (1980).
[28] M. A. Vorotyntsev and A. A. Kornyshev, Elektrokhimiya **20,** 3 (1984).
[29] M. A. Vorotyntsev, V. Yu. Izotov, A. A. Kornyshev, and W. Schmickler, Elektrokhimiya **19,** 295 (1983).
[30] V. E. Kuzema, (1982) unpublished.
[31] R. Guidelli, J. Electroanal. Chem. **123,** 59 (1981).
[32] F. H. Stillinger and A. Raman, J. Chem. Phys. **60,** 1545 (1974).
[33] S. L. Carnie and D. Y. C. Chan, J. Chem. Phys. **73,** 2949 (1980).
[34] L. Blum and D. Henderson, J. Chem. Phys. **74,** 1902 (1981).
[35] J. P. Badiali, M. L. Rosinberg, F. Vericat, and L. Blum, J. Electroanal. Chem. **158,** 253 (1983).